Spectroscopic studies of jet-cooled AgAu and Au_2

Gregory A. Bishea and Michael D. Morse
Department of Chemistry, University of Utah, Salt Lake City, Utah 84112

(Received 25 March 1991; accepted 12 July 1991)

Resonant two-photon ionization spectroscopy has been applied to the jet-cooled Au_2 and AgAu molecules. Three new band systems of Au_2 and two new systems of the poorly characterized AgAu molecule have been observed. Excited state lifetime measurements have been made, and assignments of the excited states are suggested. For Au_2 the $a\,^3\Sigma_{1u}^+ \leftarrow X\,^1\Sigma_g^+$ transition has been detected, and vibrational levels of the $a\,^3\Sigma_{1u}^+$ state have been observed up to $v' = 33$, which lies only 120 cm^{-1} below the convergence limit of the system. This allows a precise confirmation of previous high temperature Knudsen effusion measurements of the bond strength of Au_2 as $D_0^0(Au_2) = 2.290 \pm 0.008$ eV. In addition, the excited states of Au_2 of 0_u^+ symmetry are shown to have significantly shorter fluorescence lifetimes than the 1_u states, and this is explained as resulting from an admixture of Au^+Au^- ion pair character in these $\Omega' = 0_u^+$ states. The ionization potential of Au_2 has been bracketed as $IP(Au_2) = 9.20 \pm 0.21$ eV, which may be combined with the values of $D_0^0(Au_2)$ and IP(Au) to provide the dissociation energy of the Au_2^+ ion as $D_0^0(Au_2^+) = 2.32 \pm 0.21$ eV. Detailed comparisons with theoretical results are made for Au_2, and assignments of the A and B states of AgAu to $\Omega' = 0^+$ and $\Omega' = 1$, respectively, are proposed.

I. INTRODUCTION

In the preceding two papers we have presented results on the resonant two-photon ionization spectra of CuAg[1] and CuAu.[2] This work was undertaken to provide a detailed understanding of the filled d subshell transition metal dimers, so that a basis for comparison would be available when considering the question of d-orbital contributions to the chemical bonding in the open d-subshell molecules. In the present work we extend these studies to the heavier coinage metal diatomic molecules, AgAu and Au_2. In some ways an accurate knowledge of these heavier species will be more important than such a knowledge of their lighter counterparts, since the possibility of significant d-orbital contributions to the chemical bonding is greater among the $4d$ and $5d$ transition metals.[3,4] This results because there is less of a discrepancy in size between the $4d$ and $5s$ (or $5d$ and $6s$) orbitals than there is between the $3d$ and $4s$ orbitals, making the d orbitals more accessible for chemical bonding in the second and third transition metal series.[3,4]

Previous experimental work on the AgAu and Au_2 molecules has been quite limited. In two published works[5,6] Ruamps mentions band spectra of AgAu, but no analyses or listings of band positions are provided. As far as we can determine, the only other experimental work on this molecule consists of the mass spectrometric determination of the bond strength by Ackerman, Stafford, and Drowart in 1960.[7] Previous work on Au_2 has been somewhat more thorough. For example, the bond strength of this molecule has been measured by high temperature mass spectrometry many times,[7–13] making it among the best known of the bond strengths measured by this technique. In addition, the A–X[6,14–17] and B–X[6,14,16] band systems of Au_2 are well known, and both vibrational and rotational[16,17] analyses have been provided. Absorption spectra of gold clusters isolated in a low temperature argon matrix have also been reported,[18] with specific features at 365, 317, 208, and 198 nm assigned to Au_2.

Theoretical investigations of AgAu have been almost totally lacking; to our knowledge only three studies exist.[19–21] These provide information about the ground states of AgAu,[19–21] $AgAu^+$,[21] and $AgAu^-$.[20,21] Diatomic gold has been subjected to a much more complete theoretical investigation, since both the ground state[19–23] and several excited electronic states[24,25] have been studied. Following presentation of our experimental results, a comparison to these theoretical findings will be made.

Experimental details are provided in Sec. II, followed by a presentation of results in Sec. III. Section IV then provides a discussion of these results and a comparison to previous theoretical work, while Sec. V concludes the paper with a summary of our most important findings.

II. EXPERIMENT

The spectra of AgAu and Au_2 were investigated using the resonant two-photon ionization apparatus described in the previous two papers in this Journal, where results on CuAg[1] and CuAu[2] are reported. A metal target consisting of Cu, Ag, and Au in equimolar proportions, approximately 2 mm in thickness and 2.5 cm in diameter, prepared as described in the preceding paper,[2] was used for production of diatomic AgAu. This was also used for studies of CuAu,[2] Cu_2Au, and CuAgAu. Because the bond strength of AgAu is weaker than either CuAu or Au_2, this source was not ideal for the preparation of the diatomic AgAu molecule (see Sec. IV E), but it was, nevertheless, adequate for the observation of two band systems in this molecule. A 1:1 or 2:1 alloy of Ag:Au would probably be much better for the production of AgAu. A 99.95% pure gold foil ($25 \times 25 \times 0.5$ mm, Alfa Products) was used for the studies of Au_2. Both targets were used in a rotating disk vaporization assembly similar to that described by O'Brien *et al.*[26] Pulsed laser vaporization of the

0021-9606/91/205646-14$03.00

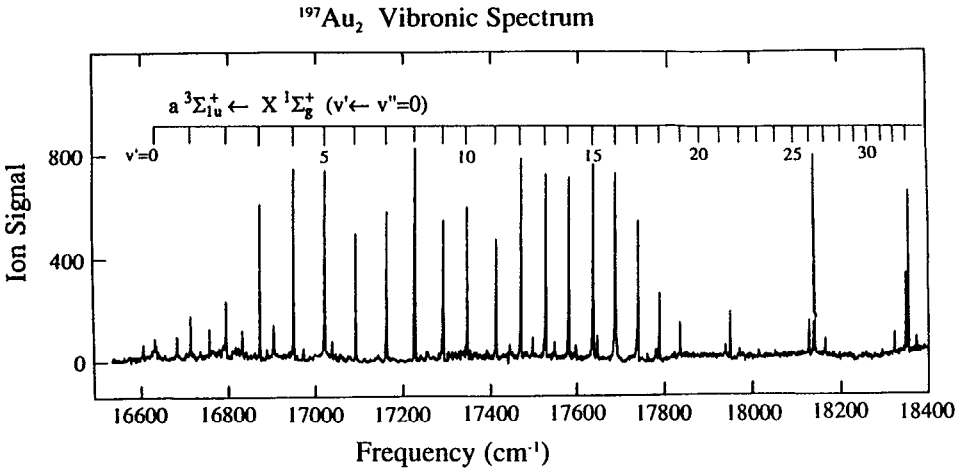

FIG. 1. Low resolution scan of the $a\,^3\Sigma_{1u}^+$–$X\,^1\Sigma_g^+$ system of $^{197}Au_2$, recorded using rhodamines 640, 610, and 590, and their mixtures, fluorescein 548, and coumarin 540A dye laser radiation in combination with an F_2 excimer laser (157 nm, 7.90 eV) for photoionization.

sample was achieved using the frequency-doubled output from a Q-switched Nd:YAG laser (532 nm, 15 mJ/pulse, focussed to a diameter of approximately 0.5 mm). The ejected atoms were then entrained in a pulsed flow of helium (120 psi), which enabled dimers and trimers to form through three-body collisions. The metal clusters then expanded supersonically into vacuum, with significant cooling of their internal degrees of freedom.

The resulting molecular beam entered a reflectron time-of-flight mass spectrometer through a 5 mm skimmer. Excitation of the AgAu and Au_2 diatomic molecules was accomplished with a pulsed dye laser counterpropagating along the molecular beam path. Following excitation, a pulsed excimer laser operating on ArF (193 nm, 6.42 eV) or F_2 (157 nm, 7.90 eV) crossed the molecular beam to ionize the excited molecules. The resulting ions were extracted and passed through a reflectron time-of-flight mass spectrometer. Detection was accomplished with a dual microchannel plate detector, the signal was digitized, and further signal processing was performed using a DEC LSI-11/73 microcomputer. The optical spectra of $^{107}Ag^{197}Au$ and $^{109}Ag^{197}Au$ were then obtained by separately monitoring the ion signals at mass 304 and 306, respectively, as a function of dye laser frequency. In the studies of diatomic gold only one isotopic form was present, and all of the reported spectra refer to $^{197}Au_2$.

Unlike the studies of CuAg[1] and CuAu[2] presented in the preceding papers, the AgAu and Au_2 molecules were not investigated with rotational resolution. The rotational structure of these heavy molecules simply could not be resolved with the 0.04 cm^{-1} laser bandwidth available to us in the present experiments. A few of the bands observed for AgAu were investigated at 0.04 cm^{-1} resolution, however, with the goal of accurately measuring the splitting between the $^{107}Ag^{197}Au$ and $^{109}Ag^{197}Au$ isotopic modifications. In some of these scans the fundamental radiation emitted by the dye laser was Raman shifted in high pressure H_2, and the first Stokes output light was used to record the absorption spectrum of I_2 for calibration.[27] This was possible because the Raman shifting process takes place in a stimulated manner, and only occurs on the Raman transition with the highest gain. For H_2 this is the $Q(1)$ line, giving a precisely defined Raman shift of 4155.264 cm^{-1}, according to the spectroscopic constants of Huber and Herzberg.[28] For bands recorded with I_2 calibration spectra the band origins are know to an accuracy of about 0.1 cm^{-1}.

Excited state lifetimes were measured by the time-delayed resonant two-photon ionization method. The resulting decay curves were fitted to exponential decay functions by a nonlinear least-squares algorithm,[29] allowing the upper state lifetimes to be extracted. For short lived levels of the A (0^+ ?) state of AgAu and the $A\,0_u^+$ and $B\,0_u^+$ states of Au_2 a convolution of a pure exponential decay with a Gaussian instrument function (FWHM of 15 ns) representing the convoluted dye and excimer laser pulses was included in the fitting function. This was required to obtain a reasonable fit to the data.

III. RESULTS

A. Diatomic gold, Au_2

1. The $a\,^3\Sigma_{1u}^+ \leftarrow X\,^1\Sigma_g^+$ system of Au_2

Figure 1 displays the lowest frequency band system that has been observed in Au_2, which is labeled as $a\,^3\Sigma_{1u}^+$–$X\,^1\Sigma_g^+$, and has been previously discussed.[30] This system was observed using F_2 radiation (157 nm, 7.90 eV) as the photoionization laser, but could not be observed using ArF radiation (193 nm, 6.42 eV). The next band system, labeled as the $A'\,1_u \leftarrow X\,^1\Sigma_g^+$ system, also appears at the high frequency end of this figure. The extended a–X band system shown in Fig. 1 is quite striking, having a vibrational frequency which is approximately 1/2 of that found for any other band system of Au_2. In addition, the large number of bands observed in this system demonstrates that the excited state bond length differs greatly from that of the ground state. Perhaps most striking is the long lifetime of the upper state of this band system, which is measured by time-delayed resonant two-photon ionization methods to be about 40 μs. Assuming that the a state decays entirely by fluorescence to the ground state, this value implies an absorption oscillator strength for the a–X system of $f \approx 1.4 \times 10^{-4}$, making the a–X system an exceedingly weak transition. Taken as a whole, these observations suggest that the upper state of the a–X system is primarily triplet ($S = 1$) in character, and that the bond order is small (or perhaps nominally zero) for this state.

TABLE I. Vibronic bands of $^{197}Au_2$.[a]

System	Band	Frequency (cm^{-1})[b]	Lifetime (μs)[c]	Band	Frequency (cm^{-1})[b]	Lifetime (μs)[c]
$a\,^3\Sigma_{1u}^+$–$X\,^1\Sigma_g^+$	0–0	16 629.69(175)		22–0	17 972.16(108)	
	1–0	16 712.37(− 11)		23–0	18 014.62(137)	
	2–0	16 792.77(− 116)		26–0	18 127.31(− 384)	
	3–0	16 871.27(− 117)		32–0	18 323.24(− 41)	
	4–0	16 947.18(− 101)		33–0	18 349.65(41)	
	5–0	17 020.97(− 36)		2–1	16 602.39(− 60)	
	6–0	17 092.78(77)		3–1	16 680.78(− 73)	
	7–0	17 161.76(140)		4–1	16 756.68(− 58)	
	8–0	17 227.86(134)		5–1	16 830.59(19)	
	9–0	17 291.38(79)	43.2(19)	6–1	16 901.63(55)	
	10–0	17 352.61(− 8)		7–1	16 970.60(117)	
	11–0	17 412.54(− 38)	36.0(6)	8–1	17 037.17(158)	
	12–0	17 470.72(− 64)		15–1	17 444.44(− 139)	
	13–0	17 527.10(− 100)		16–1	17 496.73(− 114)	
	14–0	17 582.52(− 70)		17–1	17 547.60(− 83)	
	15–0	17 636.13(− 63)		18–1	17 596.94(− 62)	
	16–0	17 688.30(− 50)		19–1	17 645.36(7)	
	17–0	17 739.22(− 14)		20–1	17 692.00(38)	
	18–0	17 788.81(31)		21–1	17 737.16(58)	
	19–0	17 836.86(64)		22–1	17 780.75(61)	
	20–0	17 883.50(94)		23–1	17 823.21(89)	
	21–0	17 928.65(114)				
$A'\,1_u$–$X\,^1\Sigma_g^+$	0–0	18 130.84(36)		0–1	17 939.42(− 43)	
	1–0	18 346.35(− 5)	4.00(2)	1–1	18 156.02(25)	
	2–0	18 555.16(52)		2–1	18 363.30(− 73)	
	3–0	18 754.39(− 84)	4.79(23)	3–1	18 565.50(90)	
$A\,0_u^+$–$X\,^1\Sigma_g^+$	0–0	19 643.20(23)	0.075(1)	0–1	19 453.43(− 15)	
	1–0	19 783.85(− 113)		1–1	19 595.88(30)	
	2–0	19 925.13(− 90)	0.078(2)	2–1	19 737.40(76)	
	3–0	20 066.79(67)		3–1	19 877.84(111)	
	4–0	20 206.42(117)		4–1	20 015.57(− 28)	
	5–0	20 343.70(29)		5–1	20 151.80(− 221)	
	6–0	20 480.25(− 36)		6–1	20 291.10(− 12)	
	7–0	20 616.40(− 45)		7–1	20 428.03(58)	
	8–0	20 752.59(47)				
$B'(1_u?)$–$X\,^1\Sigma_g^+$	0–0	23 993.40(100)	0.601(5)	0–1	23 802.22(35)	0.523(23)
	1–0	24 116.23(− 60)		1–1	23 925.21(− 110)	
	2–0	24 238.31(− 60)	0.592(5)	2–1	24 047.29(− 110)	
	3–0	24 359.30(65)		3–1	24 169.31(120)	
	4–0	24 476.76(74)		4–1	24 286.65(116)	
	5–0	24 589.51(− 153)		5–1	24 399.19(− 133)	
	6–0	24 705.34(163)		6–1	24 513.90(71)	
	7–0	24 813.73(− 30)		7–1	24 622.45(− 106)	
	8–0	24 920.77(− 124)		8–1	24 731.93(45)	
	9–0	25 028.48(85)		9–1	24 837.79(70)	
	10–0	25 130.27(− 61)				
$B\,0_u^+$–$X\,^1\Sigma_g^+$	0–0	25 683.54(97)	0.018(1)	6–0	26 738.88(− 12)	
	1–0	25 860.83(− 30)		0–1	25 491.55(− 68)	
	2–0	26 038.39(− 31)	0.019(1)	1–1	25 670.81(2)	
	3–0	26 215.97(70)		2–1	25 848.16(− 20)	
	4–0	26 389.90(− 94)		3–1	26 024.73(− 20)	
	5–0	26 565.42(1)		4–1	26 201.55(106)	

[a]Vibronic bands for $^{197}Au_2$ were fitted to the formula $\nu = \nu_{00} + \omega_e' v' - \omega_e' x_e' (v'^2 + v') + \omega_e' y_e' (v'^3 + 3v'^2/2 + 3v'/4) + \omega_e' z_e' (v'^4 + 2v'^3 + 3v'^2/2 + v'/2) - v'' \Delta G_{1/2}''$ for $v'' = 0,1$. For all band systems except the $a\,^3\Sigma_{1u}^+$–$X\,^1\Sigma_g^+$ system the higher-order anharmonicities $\omega_e' y_e'$ and $\omega_e' z_e'$ were set to zero. The resulting fitted values, with errors given in parentheses corresponding to 1σ in the least-squares fit, are: *a–X*: $\nu_{00} = 16\,627.94(78)$; $\omega_e' = 87.82(38)$; $\omega_e' x_e' = 1.689(48)$; $\omega_e' y_e' = 0.0320(22)$; $\omega_e' z_e' = -0.000\,384(33)$; $\Delta G_{1/2}'' = 190.93(36)$. *A'–X*: $\nu_{00} = 18\,130.48(64)$; $\omega_e' = 223.59(119)$; $\omega_e' x_e' = 3.84(29)$; $\Delta G_{1/2}'' = 190.62(58)$. *A–X*: $\nu_{00} = 19\,642.97(59)$; $\omega_e' = 142.97(38)$; $\omega_e' x_e' = 0.481(43)$; $\Delta G_{1/2}'' = 189.39(47)$. *B'–X*: $\nu_{00} = 23\,992.40(63)$; $\omega_e' = 126.78(31)$; $\omega_e' x_e' = 1.176(29)$; $\Delta G_{1/2}'' = 190.53(48)$. *B–X*: $\nu_{00} = 25\,682.58(50)$; $\omega_e' = 179.56(43)$; $\omega_e' x_e' = 0.498(64)$; $\Delta G_{1/2}'' = 190.35(45)$. For the *a–X* system the vibrational numbering of the *a* state is uncertain. The constants reported for this system may therefore require revision when the vibration numbering is made definite.

[b]Following each observed frequency, the residual $\nu_{obs} - \nu_{calc}$ is given in units of 0.01 cm^{-1} in parentheses.

[c]Errors reported for lifetimes correspond to 1σ in the nonlinear least-squares fit.

The large number of bands observed in this system permits a vibrational fit including higher anharmonicity corrections to be performed. The results of such a fit are given in Table I, which provides frequencies for all of the observed bands of Au_2, along with fitted vibrational constants, deviations between the measured and fitted values, and measured excited state lifetimes. With the inclusion of anharmonic terms up to $\omega_e' z_e' (v' + 1/2)^4$, an excellent fit is obtained. Using the constants so obtained, the highest bound vibrational level of the a state is predicted to occur at an energy 2.290 eV above the $v'' = 0$ level of the ground $X\,^1\Sigma_g^+$ state of the molecule. This agrees extremely well with the accepted bond strength of Au_2 determined by high temperature mass spectrometric studies of the dimerization equilibrium (2.292 ± 0.019 eV),[11] demonstrating that the a state dissociates to ground state gold atoms. Since only the ground $X\,^1\Sigma_g^+$ state and an excited $^3\Sigma_u^+$ state derive from this separated atom limit, the observed transition must be the $a\,^3\Sigma_u^+ \leftarrow X\,^1\Sigma_g^+$ transition. Furthermore, since the $a\,^3\Sigma_u^+$ state derives from the $5d_A^{10}5d_B^{10}\sigma_g^1\sigma_u^{*1}$ molecular configuration, which has a formal bond order of zero, this is entirely consistent with the low vibrational frequency found for the upper state of this system.

The $a\,^3\Sigma_u^+$ state possesses two components, described by $\Omega' = 0_u^-$ and 1_u. Presumably the same spin–orbit interactions which contaminate the $a\,^3\Sigma_u^+$ state and make it observable also serve to split these two Ω' components in energy, thereby taking the $a\,^3\Sigma_u^+$ state from Hund's case (b) to case (a), and making Ω' a good quantum number. Under such conditions the $0_u^- \leftarrow X\,^1\Sigma_g^+$ subbands are rigorously forbidden under electric dipole selection rules, and the observed system consists of the $a\,^3\Sigma_{1u}^+ \leftarrow X\,^1\Sigma_g^+$ subbands only.

As may be seen in Fig. 1, the higher members of the a–X system become progressively weaker as one goes beyond the 15–0 band. However, above 18 000 cm^{-1} another band system begins, and the 0–0 and 1–0 bands of this new system exhibit extra features. This is particularly clear for the 1–0 band, which appears to be doubled, with an extra feature nearly one-half of its intensity just a few wavenumbers below it in frequency. Careful examination of some of these extra features shows that they fit into the a–X progression as the 26–0, 32–0, and 33–0 bands. It seems clear that these particular bands have greater intensity than would be expected because they are located close in energy to the $v' = 0$ and $v' = 1$ levels of the A' state (see below), and borrow intensity from the somewhat more allowed A'–X band system. One would also expect to observe level shifts associated with this perturbation, but this requires a good estimate of the unperturbed energy levels; this is not possible without more accurate measurements of the $v' = 0$–19 levels of the $a\,^3\Sigma_u^+$ state. Some of the other extra features observed in the 17 900–18 500 cm^{-1} range correspond instead to hot bands of the A'–X system and are not related to the a–X system discussed here.

One final *caveat* concerning this band system must be mentioned: The numbering of the vibrational levels of this system is by no means certain. The difficulty here is that the apparent 0–0 band is quite weak, and it is not clear that a weaker band lying to the red of this band would be observable. In addition, gold has only one naturally occurring isotope, so it is not possible to measure an isotope shift and use this information to obtain an absolute vibrational numbering. Because of these difficulties it is not possible to determine the well depth for the $a\,^3\Sigma_{1u}^+$ state, although a lower limit on this quantity is derived in Sec. IV A. Likewise, the vibrational constants reported for the a state may require reevaluation if an absolute vibrational assignment is obtained at some time in the future.

2. The $A'\,1_u \leftarrow X\,^1\Sigma_g^+$ system of Au_2

The next band system of Au_2, shown in Fig. 2, is not nearly as extensive as the a–X system, displaying a vibrational progression only up to the 3–0 and 4–1 bands. This system, like the a–X system, can only be observed using F_2 radiation (157 nm, 7.90 eV) for photoionization, and is invisible using ArF radiation (193 nm, 6.42 eV). Based on the limited progression observed, the A' state bond length must be only slightly longer than that of ground state Au_2. The vibrational frequency of this previously unobserved upper state, given by $\omega_e' = 223.59 \pm 1.19$ cm^{-1}, is the highest yet found for any state of Au_2. The decay lifetime measured for this state is approximately 4 μs, which corresponds to an absorption oscillator strength of $f \approx 0.001$, assuming that the only decay mechanism is fluorescence to the ground electronic state.

Although one would think that there would be nothing else which could be stated about the A' state in the absence of a rotationally resolved spectrum, we can, nevertheless, identify the A' state as possessing $\Omega' = 1_u$. This determination follows from the observation that the $a\,^3\Sigma_u^+$ state borrows intensity from the A' state. Since the $\Omega' = 0_u^-$ component of the $a\,^3\Sigma_u^+$ state is optically inaccessible from the ground $X\,^1\Sigma_g^+$ state under electric dipole selection rules *in all circumstances*, it must be the $\Omega' = 1_u$ component of the $a\,^3\Sigma_u^+$ state which borrows intensity from the A' state. This implies that the A' state is in turn characterized as an $\Omega' = 1_u$ state.

3. The $A\,0_u^+ \leftarrow X\,^1\Sigma_g^+$ system of Au_2

The $A\,0_u^+ \leftarrow X\,^1\Sigma_g^+$ band system of Au_2, which has been previously observed in several investigations,[6,14–17] is shown in Fig. 3. Again, this system could only be observed using F_2 excimer radiation (157 nm, 7.90 eV) for photoionization, and could not be detected using ArF excimer radiation (193 nm, 6.42 eV). The 0–0 and 1–1 bands of this system have been rotationally resolved in a recent study by Simard and Hackett,[17] and the 2–0 and 3–0 bands have been rotationally resolved in a previous investigation by Ames and Barrow.[16] From this work it has been conclusively shown that the system is an $\Omega' = 0_u^+ \leftarrow X\,^1\Sigma_g^+$ transition. Our fitted constants of $\nu_{00} = 19\,642.97 \pm 0.59$ cm^{-1}, $\omega_e' = 142.97 \pm 0.38$ cm^{-1}, $\omega_e' x_e' = 0.481 \pm 0.043$ cm^{-1}, and $\Delta G_{1/2}'' = 189.39 \pm 0.47$ cm^{-1} are in excellent agreement with those reported by Ruamps[6] ($\omega_e' = 142.3$ cm^{-1}, $\omega_e' x_e' = 0.445$ cm^{-1}, and $\Delta G_{1/2}'' = 190.06$ cm^{-1}) and those obtained by Simard and Hackett in their much higher resolution work[17] ($\nu_{00} = 19\,644.0019 \pm 0.0006$ cm^{-1}, ω_e'

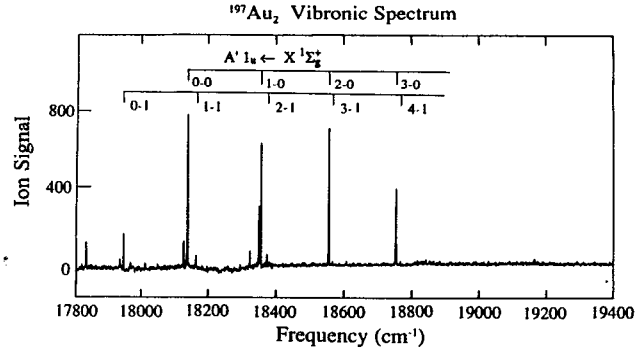

FIG. 2. Low resolution scan of the $A'\ 1_u$–$X\ ^1\Sigma_g^+$ system of $^{197}Au_2$, recorded using coumarin 540A dye laser radiation in combination with an F_2 excimer laser (157 nm, 7.90 eV) for photoionization.

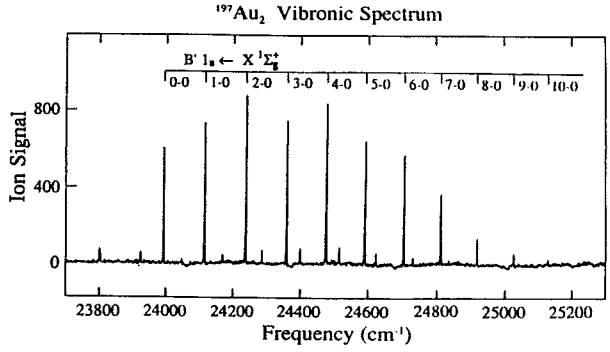

FIG. 4. Low resolution scan of the $B'\ (1_u\ ?)$–$X\ ^1\Sigma_g^+$ system of $^{197}Au_2$, recorded using stilbene 420 and exalite 398 dye laser radiation in combination with an ArF excimer laser (193 nm, 6.42 eV) for photoionization.

$= 142.61\ cm^{-1}$, $\omega_e'x_e' = 0.52\ cm^{-1}$, and $\Delta G''_{1/2} = 190.21\ cm^{-1}$).

The major new piece of information obtained in the present study is the fluorescence lifetime of the $A\ 0_u^+$ state. Measurements on the $v' = 0$ and $v' = 2$ vibrational levels of the $A\ 0_u^+$ state provide lifetimes of 75 ± 1 and 78 ± 2 ns, respectively. Assuming that the decay is dominated by fluorescence to the ground electronic state, this corresponds to an absorption oscillator strength of $f \approx 0.05$, making the A–X system very strong indeed. The great intensity of this system in both absorption and fluorescence explains why it has been observed so readily in previous investigations.

4. The $B'(1_u\ ?) \leftarrow X\ ^1\Sigma_g^+$ system of Au_2

Somewhat further to the blue another new band system of Au_2 is observed, which we have designated as the B'–X system. This is the lowest frequency band system of Au_2 which can be observed with either F_2 excimer radiation (157 nm, 7.90 eV) or ArF radiation (193 nm, 6.42 eV) as the ionization laser. The band system is displayed in Fig. 4, where a vibrational progression up to the 10–0 band has been identified. Band positions are listed in Table I, along with the fitted vibrational constants. Decay lifetimes of the $v' = 0$ and $v' = 2$ levels of the B' state have been measured by time-delayed resonant two-photon ionization methods, giving a weighted average lifetime of $\tau = 595 \pm 4$ ns. Assuming that the B' state decays entirely by fluorescence to the ground $X\ ^1\Sigma_g^+$ state, this corresponds to an absorption oscillator strength of $f \approx 0.004$. This oscillator strength is comparable to that found for the $A'\ 1_u$ state, and is sufficiently weak to explain the failure of previous investigators to observe the B'–X system.

As discussed in Sec. IV below, we have tentatively identified the B' state as possessing $\Omega' = 1_u$. This assignment is based in part on the long radiative lifetime of the B' state. As discussed in the preceding two papers,[1,2] we have found that long decay lifetimes tend to correlate with excited states of $\Omega' = 1_{(u)}$ symmetry in the diatomic coinage metals, since $\Omega' = 0_{(u)}^+$ states obtain intensity for their transitions to the ground state through mixing with ion pair states (in this case Au^+Au^-), and such covalent to ion pair excitations are among the most strongly allowed transitions which can occur. In addition, *ab initio* quantum calculations[25] of the excited states of Au_2 support the assignment of the B' state as having $\Omega' = 1_u$ symmetry.

Although we have insufficient resolution for rotationally resolved work on any of the band systems of Au_2, it is nevertheless possible to estimate the B' state bond length by a Franck–Condon analysis of the intensities of the vibrational bands. In general, we do not attempt to accurately record band intensities when we collect low-resolution spectra, and usually our spectra suffer to some degree from saturation effects. That is probably the case in the spectra of the B'–X system shown in Fig. 4. However, the hot bands originating from $v'' = 1$ of the $X\ ^1\Sigma_g^+$ state show an interesting pattern, with the 0–1, 1–1, 3–1, 4–1, 5–1, and 6–1 bands present, but with the 2–1 band barely detectable. In general, the Franck–Condon pattern of intensities arising from a $v'' = 1$ vibrational level should exhibit a single node, and the placement of this node may be used to derive the difference in bond lengths of the two states. For the pattern just described (with the 2–1 band nearly absent) this implies a bond length increase of 0.098 Å upon electronic excitation, thereby giving the B' state bond length of $r_e'[B'\ (1_u\ ?)] = 2.570$ Å. Furthermore, from the spectrum presented in Fig. 4 it is clear that the 2–1 band has less than 1/2 of the intensity of either

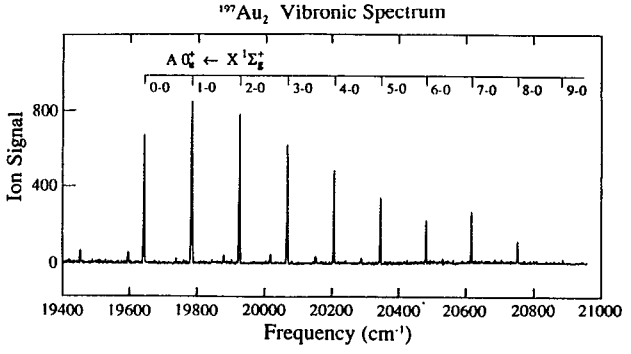

FIG. 3. Low resolution scan of the $A\ 0_u^+$–$X\ ^1\Sigma_g^+$ system of $^{197}Au_2$, recorded using coumarin 500 and 480 dye laser radiation in combination with an F_2 excimer laser (157 nm, 7.90 eV) for photoionization.

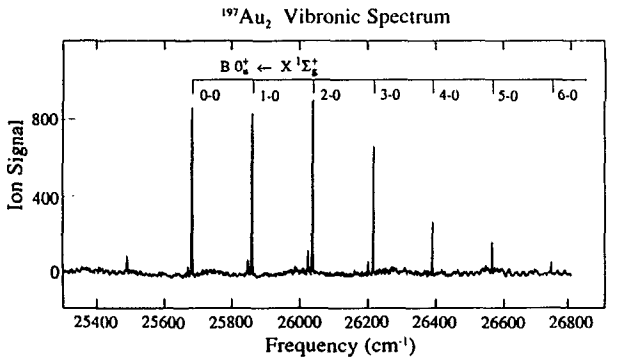

FIG. 5. Low resolution scan of the $B\,0_u^+ - X\,^1\Sigma_g^+$ system of $^{197}Au_2$, recorded using exalite 398, 389, 384, and 376 dye laser radiation in combination with an ArF excimer laser (193 nm, 6.42 eV) for photoionization.

the 1–1 or 3–1 band. This allows us to set error limits on the quoted value as $r_e'[B'\ (1_u\ ?)] = 2.570 \pm 0.017$ Å.

5. The $B\,0_u^+ \leftarrow X\,^1\Sigma_g^+$ system of Au_2

Figure 5 displays the B–X system of Au_2, which has been previously observed in several investigations.[6,14,16] Again, we find that this system may be observed using either F_2 (157 nm, 7.90 eV) or ArF (193 nm, 6.42 eV) excimer radiation as the photoionization source. Previous work has included a high resolution investigation of the B–X 0–0 band by Ames and Barrow,[16] who measured the rotational constants, obtained ground and excited state bond lengths, and were able to establish the B state as an $\Omega' = 0_u^+$ state with certainty. The fitted vibrational constants obtained in the present study ($\nu_{00} = 25\,682.58 \pm 0.50$ cm^{-1}, $\omega_e' = 179.56 \pm 0.43$ cm^{-1}, $\omega_e'x_e' = 0.498 \pm 0.064$ cm^{-1}, and $\Delta G_{1/2}'' = 190.35 \pm 0.45$ cm^{-1}) are again in excellent agreement with the results of Ruamps' work[6] ($\nu_{00} = 25\,680.4$ cm^{-1}, $\omega_e' = 179.85$ cm^{-1}, $\omega_e'x_e' = 0.680$ cm^{-1}, and $\Delta G_{1/2}'' = 190.06$ cm^{-1}) as well as with the more accurate results of Ames and Barrow[16] ($\nu_{00} = 25\,679.870 \pm 0.025$ cm^{-1}) and Simard and Hackett[17] ($\Delta G_{1/2}'' = 190.21$ cm^{-1}).

The major new piece of information which we can contribute to an understanding of the $B\,0_u^+$ state is our measurement of the excited state lifetime, which give a weighted average of 18.3 ± 0.3 ns for the $v' = 0$ and $v' = 2$ levels. Assuming that the molecular decay is dominated by fluorescence to the ground electronic state, this corresponds to an absorption oscillator strength of $f \approx 0.13$, making this one of the most strongly allowed transitions observed in any molecular system. As discussed in Sec. IV below, it is likely that the $B\,0_u^+$ state of Au_2 is best described as an ion pair state, deriving from the Au^+, $5d^{10}6s^0$, $^1S_0 + Au^-$, $5d^{10}6s^2$, $^1S_0$ limit. The great intensity of the B–X system then arises as a charge transfer transition taking the system from the covalent ground state to the ion pair state.

B. Diatomic silver–gold, AgAu

1. The $A\,(0^+\ ?) \leftarrow X\,^1\Sigma^+$ system of AgAu

Figure 6 displays the two band systems of AgAu observed in the present investigation, labeled as the A–X and B–X systems. Both were detected using ArF excimer radiation (193 nm, 6.42 eV) for photoionization. The A–X system consists of a very long progression, extending up to the 23–0 band, assuming that the vibrational numbering is correct. Although we have not been able to resolve the rotational structure of any of the bands of AgAu, high resolution scans over the 1–0, 2–0, 3–0, 4–0, and 5–0 bands have been performed, and the isotope shifts $\nu_{v'-0}(^{107}Ag^{197}Au) - \nu_{v'-0}(^{109}Ag^{197}Au)$ have been measured. The results, listed in Table II along with measured band positions and excited state lifetimes, suggest that the vibrational numbering is correct, since an extrapolation of the accurately measured isotope shifts for the 1–0 through 5–0 bands leads to a small isotope shift ($+0.24$ cm^{-1}) for the 0–0 band, opposite in sense to that observed for the 1–0 through 5–0 bands. Neglecting corrections due to anharmonicity in the X and A states, and assuming that electronic

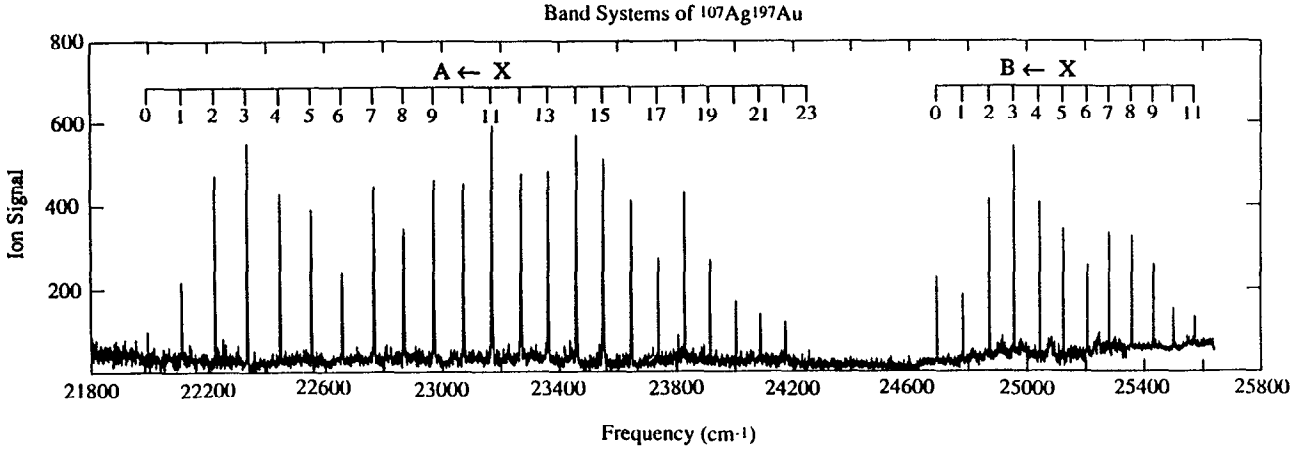

FIG. 6. Low resolution scan of the $A\,(0^+\ ?)$–$X\,^1\Sigma^+$ and $B\,(1\,?)$–$X\,^1\Sigma^+$ systems of $^{107}Ag^{197}Au$, recorded using coumarin 460, 440, stilbene 420, and exalite 398 and 389 dye laser radiation in combination with an ArF excimer laser (193 nm, 6.42 eV) for photoionization.

TABLE II. Vibronic bands of $^{107}Ag^{197}Au$.[a,b]

System	Band	Observed frequency (cm^{-1})	Isotope shift (cm^{-1})	Lifetime (μs)[c]
$A(0^+?)$–$X\,^1\Sigma^+$	0–0	21 993.50(− 248)	− 0.22	
	1–0	*22 110.18(− 4)	* − 0.35	
	2–0	*22 223.32(34)	* − 1.10	
	3–0	*22 334.85(60)	* − 1.66	
	4–0	*22 445.03(99)	* − 2.42	
	5–0	*22 553.34(99)	* − 2.90	
	6–0	22 658.45(− 72)	− 3.18	
	7–0	22 767.08(257)	− 4.21	
	8–0	22 868.51(15)	− 4.54	
	9–0	22 971.22(49)	− 5.30	
	10–0	23 072.35(73)	− 5.64	
	11–0	23 169.17(− 186)	− 5.64	
	12–0	23 270.52(158)	− 6.06	0.039(1)
	13–0	23 363.09(− 229)	− 6.73	0.039(1)
	14–0	23 460.43(10)	− 7.47	0.039(1)
	15–0	23 551.72(− 208)	− 8.53	0.041(1)
	16–0	23 647.11(133)	− 9.01	
	17–0	23 733.64(− 264)	− 7.03	
	18–0	23 826.64(135)	− 10.07	
	19–0	23 911.05(− 178)	− 8.08	
	20–0	23 999.45(58)	− 10.46	
	21–0	24 084.40(96)	− 10.33	
	22–0	24 167.77(126)	− 11.29	
	23–0	24 247.97(− 14)	− 12.96	
$B(1?)$–$X\,^1\Sigma^+$	0–0	24 693.10(61)	− 1.52	1.13(11)
	1–0	24 781.96(− 106)	− 2.38	
	2–0	24 872.23(79)	** − 2.23	0.99(8)
	3–0	24 955.84(− 190)	− 2.65	
	4–0	25 043.41(148)	** − 3.04	1.29(12)
	5–0	25 123.96(− 5)	− 4.78	1.23(8)
	6–0	25 205.75(178)	** − 3.84	1.28(44)
	7–0	25 279.88(− 194)	− 2.86	
	8–0	25 358.03(48)	− 5.20	
	9–0	25 431.93(76)	− 4.37	
	10–0	25 500.46(− 222)	− 5.19	
	11–0	25 573.34(127)	− 6.06	

[a]Asterisks indicate that the band was scanned in high resolution (0.04 cm^{-1}) to provide an accurate measurement of the isotope shift, and that the first Stokes radiation from a high pressure Raman cell was used to simultaneously record an I_2 absorption spectrum (Ref. 27) for wavelength calibration. In these scans the band origins listed are probably accurate to $\pm$ 0.1 cm^{-1}. In the remainder, the band origins listed are probably only accurate to $\pm$ 3 cm^{-1}. Double asterisks indicate isotope shifts measured in high resolution (0.04 cm^{-1}), but without absolute calibration based on the spectrum of I_2.

[b]Observed band frequencies have been fitted to the formula $\nu = \nu_{00} + v'\omega_e' - (v'^2 + v')\omega_e'x_e'$, resulting in the following values of ν_{00}, ω_e', and $\omega_e'x_e'$ (with their 1σ errors in parentheses): A–X $\nu_{00} = 21\,995.97(86)$; $\omega_e' = 115.73(18)$; $\omega_e'x_e' = 0.74(1)$. B–X $\nu_{00} = 24\,692.49(116)$; $\omega_e' = 92.65(53)$; $\omega_e'x_e' = 1.06(4)$. Residuals in the fit are given in parentheses as $\nu_{obs} - \nu_{calc}$ for each observed band in the table. Since the vibrational assignments for both the A–X and B–X systems are not absolutely certain, these constants may require revision after the vibrational assignments are made definite.

[c]The 1σ errors in the fitted lifetimes are given in parentheses.

isotope effects are absent, this extrapolated isotope shift leads to an estimate of the ground state vibrational frequency of 196 cm^{-1}. Although this value is quite reasonable, the neglect of electronic isotope effects and the possibility of isotopically dependent perturbations make the calculation of a ground state frequency by this method perilous at best.

Measured decay lifetimes for the $v' = 12$, 13, 14, and 15 levels of the A state of AgAu fall within the range of 38.7 to 41.1 ns, with a weighted average of 39.4 $\pm$ 0.3 ns. Assuming that the decay is dominated by fluorescence to the ground electronic state, this implies an absorption oscillator strength of $f \approx 0.08$ for the A–X system, making it an intense transition indeed. Based on the ideas presented in the preceding two papers[1,2] and the results found for Au_2 above, the intensity of the A–X band system provides a strong argument for assigning the A state as having $\Omega' = 0^+$ character. Moreover, the oscillator strength for this system is so great that it seems likely that the A state is best described as an ion pair state, correlating to the Ag^+Au^- ionic limit, as is discussed more fully in Sec. IV below.

2. The $B(1?) \leftarrow X\,^1\Sigma^+$ system of AgAu

To the blue of the A–X system of AgAu shown in Fig. 6 is another system, designated as the B–X system. Although not as extended as the A–X system, a vibrational progression is nevertheless observed up to the 11–0 band. In addition to being not quite as extended as the A–X system, the apparent origin band of the B–X system is relatively strong. Both of these observations are consistent with the B state having a bond length which is intermediate between that of the X and A states. An anomaly exists, however, in that the accurately measured isotope shifts of the 2–0, 4–0, and 6–0 bands are too large. Extrapolating from these bands to the apparent origin band, one finds that an isotope shift of $\nu_{v'-0}(^{107}Ag^{197}Au) - \nu_{v'-0}(^{109}Ag^{197}Au) = -1.43\ cm^{-1}$ is predicted. This is in agreement with the value of $-1.52\ cm^{-1}$ measured in low resolution, but is *not* consistent with the assignment of the first observed feature to an origin band in a molecule which is free of isotopically dependent perturbations and electronic isotope effects. If no unusual perturbations or electronic isotope effects are present, the isotope shift information suggests that the first observed band should be renumbered as the 4–0 band instead of the 0–0 band. Although this does not seem likely based on the relative intensities of the observed features, it cannot be totally ruled out at present.

Excited state lifetimes have been measured for the $v' = 0, 2, 4, 5$, and 6 levels of the B state of AgAu, resulting in an average value of $\tau = 1.14 \pm 0.05\ \mu s$. This long lifetime corresponds to an absorption oscillator strength of $f \approx 0.002$, which is reduced considerably from that obtained for the A–X system. Based on considerations outlined in the previous papers on CuAg[1] and CuAu,[2] it seems likely that subsequent high resolution work will find the B state of AgAu to possess $\Omega' = 1$.

IV. DISCUSSION

A. The ground $X\,^1\Sigma_g^+$ and $a\,^3\Sigma_u^+$ states of Au_2

In this work we have determined rather little new information about the ground state of Au_2. From the observation that the a–X, A'–X, and A–X systems require 7.90 eV photons for the second ionization step, while the B'–X and B–X systems may be observed using either 7.90 or 6.42 eV photons, however, we are able to bracket the ionization potential of Au_2 in the range of 8.99 to 9.40 eV, or $IP(Au_2) = 9.20 \pm 0.21$ eV. This is quite a bit larger than the calculated value obtained by Partridge, Bauschlicher, and Langhoff (8.63 eV), but is close to their recommended scaled value of 9.41 eV.[21] Within the error of the measurement, the value of $IP(Au_2)$ determined through this work is identical to the accepted ionization potential of atomic gold, given as $IP(Au) = 9.226$ eV.[31] Since it is easily shown through a thermodynamic cycle that $D_0^0(Au_2^+) = D_0^0(Au_2) + IP(Au) - IP(Au_2)$, this implies that the bond strengths of Au_2 and Au_2^+ are equal to within the uncertainty of the ionization potential measurements.

In addition to bracketing the value of $IP(Au_2)$, our measurements of the vibrational levels of the $a\,^3\Sigma_{1u}^+$ state may be extrapolated to obtain an accurate measure of the bond strength of diatomic gold, $D_0^0(Au_2)$. Since levels up to $v' = 33$ have been directly observed, the vibrational constants of the $a\,^3\Sigma_{1u}^+$ state are relatively well determined, and the dissociation energy may be determined by simply extrapolating the energies of higher vibrational levels until the convergence limit is reached. Such a process leads to $D_0^0(Au_2) = 2.290$ eV, with the last observed vibrational level of the $a\,^3\Sigma_{1u}^+$ state lying at 2.275 eV. A conservative estimate of the error in this extrapolation is taken as 1/2 of the energy difference between the last observed level and the projected limit, giving $D_0^0(Au_2) = 2.290 \pm 0.008$ eV. This is in essentially exact agreement with the results of the best high temperature Knudsen effusion mass spectrometric studies, which give $D_0^0(Au_2) = 2.292 \pm 0.019$ eV.[11]

Finally, the $a\,^3\Sigma_{1u}^+$ state of Au_2 has been shown to be optically accessible from the ground $X\,^1\Sigma_g^+$ state, although the oscillator strength of the a–X system is only $f \approx 1.4 \times 10^{-4}$. This nevertheless implies some spin–orbit contamination of the $a\,^3\Sigma_{1u}^+$ state through mixing with a $^1\Pi_u$ state, probably deriving from the $d^{10}s^1$, $^2S + d^9s^2$, ^2D or $d^{10}s^1$, $^2S + d^{10}p^1$, $^2P^0$ limits. Although the $v' = 0$ level of the $a\,^3\Sigma_{1u}^+$ state has not been located with certainty, the observed levels indicate that the $v' = 0$ level of the $a\,^3\Sigma_{1u}^+$ state is bound by at least $1840\ cm^{-1}$.

B. The $d_A^9 d_B^{10} \sigma_g^2 \sigma_u^{*1}$ states of Au_2

An understanding of the electronic structure of the remaining excited states of diatomic gold, summarized in Table III, is best obtained by considering the separated atom limits listed in Table IV. Aside from the $a\,^3\Sigma_u^+$ state discussed above, all of the observed excited electronic states correlate to excited separated atom limits. From the data presented in Table III the well depths, D_e', of the observed excited states of Au_2 may be estimated by assuming that they follow a Morse function behavior, giving $D_e' = \omega_e'^2/4\omega_e'x_e'$. This may be converted to D_0 by subtracting the excited state zero-point energy, and from this value the energy of the separated atom limit of the excited state, E_{SA}, may be derived by adding the frequency of the origin band, ν_{00}, and subtracting the bond strength of the ground state, D_0^0, to give

$$E_{SA} = \omega_e'^2/4\omega_e'x_e' - \omega_e'/2 + \omega_e'x_e'/4 + \nu_{00} - D_0^0. \tag{4.1}$$

This very approximate analysis places the dissociation limits of the $A'\,1_u$, $A\,0_u^+$, $B'\,(1_u?)$, and $B\,0_u^+$ excited states of Au_2 2800, 11 725, 8875, and 23 300 cm^{-1} above ground state atoms, respectively.

With the exception of the $B\,0_u^+$ state, the only separated atom limit in the vicinity of these crude predictions is the $d^{10}s^1$, $^2S_{1/2} + d^9s^2$, $^2D_{5/2}$ limit at 9161.30 cm^{-1}. From this limit three excited states arise which are optically accessible in Hund's case (c) through electric dipole transitions from the ground state. These are one 0_u^+ state and two 1_u states, in exact correspondence with the $A'\,1_u$, $A\,0_u^+$, and $B'\,(1_u?)$ states. Accordingly, these three states are assigned as corre-

TABLE III. Electronic states of $^{197}Au_2$.[a]

State	T_0 (cm^{-1})	ω_e (cm^{-1})	$\omega_e x_e$ (cm^{-1})	B_e (cm^{-1})	α_e (cm^{-1})	r_e (Å)	Lifetime (μs)
$B\,0_u^+$	25 679.870(25)[b]	179.85[j]	0.68[j]	0.026 961(7)[b,c]		2.5197(3)[b,d]	0.018(1)[e]
$B'(1_u?)$[g]	23 992.4(6)[e]	126.8(3)[e]	1.18(3)[e]			2.570(17)[e]	0.595(3)[e]
$A\,0_u^+$	19 644.0019(6)[f]	142.61[f]	0.52[f]	0.025 979(36)[f]	0.000 095(16)[f]	2.5669(18)[f]	0.076(1)[e]
$A'1_u$[h]	18 130.5(6)[e]	223.6(12)[e]	3.84(29)[e]				4.5(5)[e]
$a\,^3\Sigma_u^+(1_u)$	16 627.9(8)[e,i]	87.8(4)[e,i]	1.69(5)[e,i]				40(4)[e]
$X\,^1\Sigma_g^+$	0.0	190.9[j]	0.420[j]	0.028 022[f]	0.000 066[f]	2.4715[f]	...

[a]Uncertainties are given in parentheses as one standard deviation. $D_0^0(Au_2) = 2.290(8)$ eV; $IP(Au_2) = 9.20(21)$ eV; $D_0^0(Au_2^+) = 2.32(21)$ eV.
[b]From Ref. 15.
[c]This value is B_0, not B_e.
[d]This value is r_0, not r_e.
[e]This work.
[f]From Ref. 17.
[g]Assignment based on comparisons with theoretical work of Refs. 24 and 25.
[h]Assignment based on the observation that the $a\,^3\Sigma_u^+(1_u)$ state borrows intensity from the A' state.
[i]Vibrational constants for the $a\,^3\Sigma_u^+(1_u)$ state may require revision when the vibrational numbering of this state becomes definite. Higher anharmonicities of $\omega_e'y_e' = 0.0320(22)$ and $\omega_e'z_e' = -0.000\,384(33)$ are obtained for the $v' = 0$–23, 26, 32, and 33 levels of this state.
[j]From Ref. 6.

lating to the $d^{10}s^1$, $^2S_{1/2} + d^9s^2$, $^2D_{5/2}$ limit, and have electronic configurations of $d_A^{10}d_B^9\sigma_g^2\sigma_u^{*1}$.

Two case (a) states arising from the $^2S + {}^2D$ limit generate case (c) states labeled as 0_u^+. These are the $^1\Sigma_u^+$ and $^3\Pi_u$ states, which arise from $s\sigma_u \leftarrow d\sigma_g$ and $s\sigma_u \leftarrow d\pi_g$ excitations, respectively. If the d orbitals of Au_2 are split into bonding and antibonding orbitals, then the $^3\Pi_u$ state arising from the promotion of an *antibonding* $d\pi_g$ electron into the *antibonding* $s\sigma_u$ orbital will be expected to lie lower in energy than the $^1\Sigma_u^+$ state arising from the promotion of the *bonding* $d\sigma_g$ electron to this $s\sigma_u$ *antibonding* orbital. Even if the splitting of the d orbitals into bonding and antibonding pairs is negligible, exchange effects would still place the $^3\Pi_u$ state below the $^1\Sigma_u^+$ state. For these reasons, it seems clear that the $^3\Pi_u$ ($\Omega' = 0_u^+$) state should correlate to the lower of the two $^2S + {}^2D$ limits. Accordingly, the $A\,0_u^+$ state which correlates to this limit, is expected to be primarily $^3\Pi_u$ in character. It must nevertheless have a significant admixture of $^1\Sigma_u^+$ character, however, since the $A\,0_u^+ \leftarrow X\,^1\Sigma_g^+$ transition has an oscillator strength of $f \approx 0.05$. These expectations are borne out in a recent theoretical calculation by Das and Balasubramanian,[25] who describe the $A\,0_u^+$ state as having 49% $^3\Pi_u$ ($s\sigma_u \leftarrow d\pi_g$), 21% $^1\Sigma_u^+$ ($s\sigma_u \leftarrow d\sigma_g$), and 12% $^1\Sigma_u^+$ ($s\sigma_u \leftarrow s\sigma_g$) character, where the descriptions in parentheses indicate the rearrangement of electrons required to take the ground state of Au_2 to the designated

TABLE IV. Separated atom limits in Au_2.

Separated atom limit				
Atom A	Atom B	Energy[a] (cm^{-1})	Case (c) states[b]	Case (a) states[b]
$Au^+(^1S_0)$	$Au^-(^1S_0)$	55 789.7	$0_g^+, 0_u^+$	$^1\Sigma_g^+, {}^1\Sigma_u^+$
$d^9s^2, {}^2D_{3/2}$	$d^9s^2, {}^2D_{3/2}$	42 870.60	$0_g^+(2), 0_u^-(2), 1_g, 1_u(2), 2_g, 2_u, 3_u$	$^1\Sigma_g^+(3), {}^1\Sigma_u^-(2), {}^1\Pi_g(2), {}^1\Pi_u(2), {}^1\Delta_g(2), {}^1\Delta_u, {}^1\Phi_g, {}^1\Phi_u, {}^1\Gamma_g, {}^3\Sigma_u^+(3), {}^3\Sigma_g^-(2), {}^3\Pi_u(2), {}^3\Pi_g(2), {}^3\Delta_u(2), {}^3\Delta_g, {}^3\Phi_u, {}^3\Phi_g, {}^3\Gamma_u$
$d^9s^2, {}^2D_{5/2}$	$d^9s^2, {}^2D_{3/2}$	30 596.60	$0_g^+(2), 0_u^+(2), 0_g^-(2), 0_u^-(2), 1_g(4), 1_u(4), 2_g(3), 2_u(3), 3_g(2), 3_u(2), 4_g, 4_u$	
$d^9s^2, {}^2D_{5/2}$	$d^9s^2, {}^2D_{5/2}$	18 322.60	$0_g^+(3), 0_u^-(3), 1_g(2), 1_u(3), 2_g(2), 2_u(2), 3_g, 3_u(2), 4_g, 4_u, 5_u$	
$d^{10}s^1, {}^2S_{1/2}$	$d^{10}p^1, {}^2P_{3/2}^0$	41 174.30	$0_g^+, 0_u^+, 0_g^-, 0_u^-, 1_g(2), 1_u(2), 2_g, 2_u$	$^1\Sigma_g^+, {}^1\Sigma_u^+, {}^3\Sigma_g^+, {}^3\Sigma_u^+, {}^1\Pi_g, {}^1\Pi_u, {}^3\Pi_g, {}^3\Pi_u$
$d^{10}s^1, {}^2S_{1/2}$	$d^{10}p^1, {}^2P_{1/2}^0$	37 358.90	$0_g^+, 0_u^+, 0_g^-, 0_u^-, 1_g, 1_u$	
$d^{10}s^1, {}^2S_{1/2}$	$d^9s^2, {}^2D_{3/2}$	21 435.30	$0_g^+, 0_u^+, 0_g^-, 0_u^-, 1_g(2), 1_u(2), 2_g, 2_u$	$^1\Sigma_g^+, {}^1\Sigma_u^+, {}^3\Sigma_g^+, {}^3\Sigma_u^+, {}^1\Pi_g, {}^1\Pi_u, {}^3\Pi_g, {}^3\Pi_u, {}^1\Delta_g, {}^1\Delta_u, {}^3\Delta_g, {}^3\Delta_u$
$d^{10}s^1, {}^2S_{1/2}$	$d^9s^2, {}^2D_{5/2}$	9 161.30	$0_g^+, 0_u^+, 0_g^-, 0_u^-, 1_g(2), 1_u(2), 2_g(2), 2_u(2), 3_g, 3_u$	
$d^{10}s^1, {}^2S_{1/2}$	$d^{10}s^1, {}^2S_{1/2}$	0.00	$0_g^+, 0_u^-, 1_u$	$^1\Sigma_g^+, {}^3\Sigma_u^+$

[a]Atomic energies and IP(Au) taken from Ref. 32; electron affinity taken as EA(Au) = 18 620.35 cm^{-1} from Ref. 31.
[b]From Reference 33.

excited state. Thus, in this notation the $^1\Sigma_u^+$ state designated by $(s\sigma_u \leftarrow d\sigma_g)$ is generated by removing an electron from the $d\sigma_g$ bonding orbital and transferring it to the $s\sigma_u$ antibonding orbital. The last $^1\Sigma_u^+$ component, which contributes 12% to the makeup of the $A\,0_u^+$ state, correlates diabatically in case (a) to the ion pair limit $Au^+ + Au^-$, and is probably responsible for most of the intensity of the $A \leftarrow X$ transition.

To carry this analysis further, let us assume that the $5d$ orbitals of gold *are* split into bonding and antibonding orbitals, with the orbitals falling into the energy ordering $d\sigma_g < d\pi_u < d\delta_g < d\delta_u < d\pi_g < d\sigma_u$. There is good evidence for such a splitting pattern in the calculations of Das and Balasubramanian, as is particularly obvious in the triplet manifold of states arising from the promotion of a d electron to the $s\sigma_u^*$ orbital.[25] Given this ordering of the molecular orbital energies, one would expect the triplet states arising from $s\sigma_u^* \leftarrow d$ excitations to fall in the energetic order $^3\Sigma_g^+ < {}^3\Pi_u < {}^3\Delta_g < {}^3\Delta_u < {}^3\Pi_g < {}^3\Sigma_u^+$. This is precisely what Das and Balasubramanian find when spin–orbit coupling is excluded from the calculation.[25] One would ordinarily expect the same energetic ordering for the singlet states as well, giving $^1\Sigma_g^+ < {}^1\Pi_u < {}^1\Delta_g < {}^1\Delta_u < {}^1\Pi_g < {}^1\Sigma_u^+$, however this is not the case. Within the $^1\Pi_{g,u}$ and $^1\Delta_{g,u}$ sets of states the energetic ordering given above is preserved, but the $^1\Sigma_g^+$ and $^1\Sigma_u^+$ states are out of place. In particular, the $^1\Sigma_u^+$ state, which would be expected to be the highest lying of these states, instead *lies lowest in energy*. Without a doubt this occurs because of extensive mixing due to an avoided crossing with the $^1\Sigma_u^+$ ion pair state described as $Au^+ Au^-$.

With this in mind, we may now consider the electronic structure of the $A'\,1_u$ and B' (1_u ?) states observed in the present work, which are now known to dissociate to $^2S_{1/2} + {}^2D_{5/2}$ atoms. The only Hund's case (a) states arising from the $^2S + {}^2D$ atomic limit which can generate $\Omega' = 1_u$ states are the $^3\Sigma_u^+$, $^1\Pi_u$, $^3\Pi_u$, and $^3\Delta_u$ molecular terms. Based on the bonding arguments given above, the triplets among these would be expected to fall into the energetic ordering $^3\Pi_u < {}^3\Delta_u < {}^3\Sigma_u^+$. Exchange considerations would force the $^1\Pi_u$ term to lie above its corresponding $^3\Pi_u$ term, but its placement relative to the $^3\Delta_u$ and $^3\Sigma_u^+$ terms would be dependent on the relative magnitudes of the bonding interactions between the $5d$ orbitals and the exchange interaction. With this in mind we expect that the lower lying $A'\,1_u$ state should be primarily $^3\Pi_u$ in character, and the B' (1_u ?) state should be either primarily $^1\Pi_u$ or $^3\Delta_u$ in character.

These expectations are again borne out by the theoretical work of Das and Balasubramanian,[25] who find the $A'\,1_u$ state to consist of 54% $^3\Pi_u$ $(s\sigma_u \leftarrow d\pi_g)$, 18% $^1\Pi_u$ $(s\sigma_u \leftarrow d\pi_g)$, and 8% $^3\Delta_u$ $(s\sigma_u \leftarrow d\delta_g)$ character. The next higher 1_u state calculated by these authors, which must correspond to our B' (1_u ?) state, is then found to have the composition of 43% $^1\Pi_u$ $(s\sigma_u \leftarrow d\pi_g)$, 20% $^3\Pi_u$ $(s\sigma_u \leftarrow d\pi_g)$, and 15% $^3\Sigma_u^+$ $(s\sigma_u \leftarrow d\sigma_g)$. The fact that this state is found to be primarily $^1\Pi_u$ rather than $^3\Delta_u$ in character shows that the energetic splitting of the $5d$ orbitals due to bonding interactions dominates over the exchange interactions in diatomic gold. The greater oscillator strength of the B'–X system ($f \approx 0.004$), as compared to the A'–X system ($f \approx 0.001$), also reflects the greater amount of singlet character in the B' state, and provides an experimental corroboration of the theoretical results.

C. The ion pair states of Au_2

As noted above, the extrapolated dissociation limit of the $B\,0_u^+$ state of Au_2 lies 23 300 cm^{-1} above ground state atoms. As shown in Table IV, the only separated atom asymptote in this energy range providing states of 0_u^+ symmetry is the $^2S_{1/2} + {}^2D_{3/2}$ separated atom limit. Moreover, since the only case (a) states deriving from the $^2S + {}^2D$ atomic limit and giving rise to 0_u^+ states are the $^1\Sigma_u^+$ $(s\sigma_u \leftarrow d\sigma_g)$ and $^3\Pi_u$ $(s\sigma_u \leftarrow d\pi_g)$ states, and the $A\,0_u^+$ state has already been assigned as primarily $^3\Pi_u$ $(\Omega' = 0_u^+)$ in character, it would seem that the $B\,0_u^+$ state should correspond primarily to the $^1\Sigma_u^+$ $(s\sigma_u \leftarrow d\sigma_g)$ state. This assignment presents difficulties, however, since the promotion of an electron from the *most strongly bonding* of the d-based molecular orbitals to the *antibonding* $s\sigma_u^*$ orbital should lead to a state which is the highest of the $d_A^9 d_B^{10} \sigma_g^2 \sigma_u^{*1}$ states, particularly if the remaining $d\sigma_g$ and the $s\sigma_u$ electrons are singlet coupled. Instead, this state is found to lie only about 1700 cm^{-1} above the $B'\,1_u$ state, which consists primarily of $^1\Pi_u$ $(s\sigma_u \leftarrow d\pi_g)$ character. There is no reason to expect that a state arising from excitation of a strongly bonding $d\sigma_g$ electron to lie only 1700 cm^{-1} above the corresponding state resulting from excitation of an antibonding $d\pi_g$ electron.

A second problem with the assignment of the $B\,0_u^+$ state to the $^1\Sigma_u^+$ $(s\sigma_u \leftarrow d\sigma_g)$ electronic configuration is associated with the great oscillator strength of the B–X transition. If the $B\,0_u^+$ state were primarily $^1\Sigma_u^+$ $(s\sigma_u \leftarrow d\sigma_g)$ in character, then the B–X transition would asymptotically become an $s \leftarrow d$ excitation on a single gold atom and in this limit it would be rigorously forbidden under electric dipole selection rules. In the molecule it becomes allowed of course, but its intensity would be expected to be comparable to that found for the B'–X system, which also corresponds to an $s \leftarrow d$ excitation in the separated atom limit. Our experimental results, however, show the B–X oscillator strength ($f \approx 0.13$) to be much greater than the B'–X oscillator strength ($f \approx 0.004$), thereby invalidating the assignment of the B state as primarily $^1\Sigma_u^+$ $(s\sigma_u \leftarrow d\sigma_g)$ in character.

The solution to this dilemma lies in the ion pair states correlating to the $Au^+, {}^1S_0 + Au^-, {}^1S_0$ separated ion limit. Although this limit lies 55 790 cm^{-1} above ground state atoms, the long range Coulomb attraction between ions has the effect of reducing this energy considerably, and brings the ion pair state into the energy range of the $B\,0_u^+$ state. This is displayed in Fig. 7, which shows the experimentally derived potential energy curves for the X, a, A', A, B', and B states of Au_2, along with the separated atom limits. The dashed curve which is displayed is extrapolated from the $Au^+ + Au^-$ separated ion limit using a $-e^2/R$ attractive potential. No additional attractive interactions due to ion polarization effects or repulsive interactions due to Pauli re-

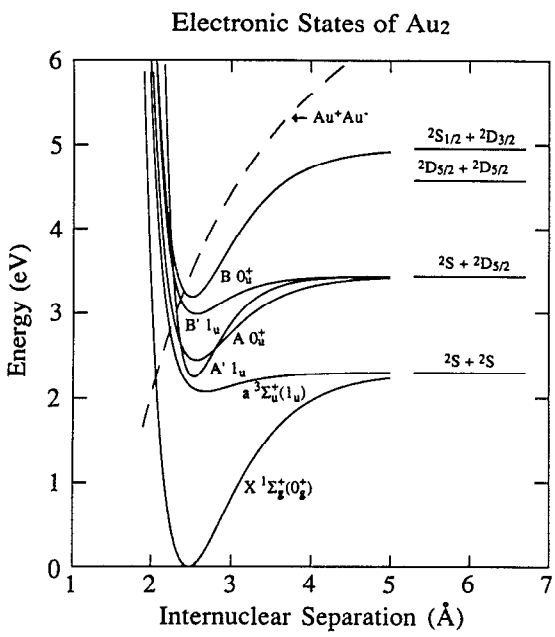

FIG. 7. Qualitative potential energy curves for the experimentally known electronic states of Au_2. Bond lengths, vibrational frequencies, and electronic energies are taken from Table III. Potential curves are plotted as Morse potentials, with anharmonicities adjusted to force dissociation to the appropriate separated atom limits. The ion pair curve for Au^+Au^- is plotted as a dashed line, without any corrections to account for the polarizability of one ion in the field of the other, or for Pauli repulsion at short distances. Owing to its intensity in absorption the $B\,0_u^+$ state is thought to correspond to the ion pair state Au^+Au^-.

pulsions of the filled orbitals are included. The dashed curve therefore displays the unphysical behavior of approaching $-\infty$ as $R \to 0$, while the real ion pair state curves would turn up and become repulsive as R is decreased beyond some value. Nevertheless, the dashed curve provides a useful guide in determining the approximate energy range in which ion pair states might be expected to occur. As is evident in Fig. 7, the Au^+Au^- ion pair curve parallels the $B\,0_u^+$ state quite closely, and only a small energy correction due to ion polarizability is necessary to shift the dashed curve over to the $B\,0_u^+$ curve.

In the nomenclature of molecular orbital configurations, the relevant filled d subshell states of Au_2 are the σ_g^2, $X\,^1\Sigma_g^+$ ground state, the $\sigma_g^1\sigma_u^1$, $a\,^3\Sigma_u^+$ state which is nominally repulsive, the $\sigma_g^1\sigma_u^1$, $^1\Sigma_u^+$ state, and the σ_u^2, $^1\Sigma_g^+$ state. The first two of these correlate to ground state $^2S_{1/2} + {}^2S_{1/2}$ atoms, while the last two states correlate to the separated ion limit of Au^+, $^1S_0 + Au^-$, $^1S_0$. By considering the orbital energies it is clear that the $\sigma_g^1\sigma_u^1$, $^1\Sigma_u^+$ ion pair state should lie below the σ_u^2, $^1\Sigma_g^+$ ion pair state, and in any case it is the $\sigma_g^1\sigma_u^1$, $^1\Sigma_u^+$ ion pair state which should be considered as a possible configuration of the $B\,0_u^+$ state. An assignment of the $B\,0_u^+$ state to this configuration would make the B–X system an extremely allowed $s\sigma_u \leftarrow s\sigma_g$ transition, and would be entirely in keeping with all of the experimental observations regarding this state. This assignment is verified in the *ab initio* calculations of Das and Balasubramanian,[25] who find the $B\,0_u^+$ state to consist of 49% $^1\Sigma_u^+$ ($s\sigma_u \leftarrow s\sigma_g$) (ion pair) character, along with 33% $^3\Pi_u$ ($s\sigma_u \leftarrow d\pi_g$) character. This is also supported by previous work by Ermler, Lee, and Pitzer,[24] who show the $Au^+ + Au^-$ ion pair state undergoing an avoided crossing with the 0_u^+ state arising from the $^2S_{1/2} + {}^2D_{3/2}$ limit. The lower curve, which carries ion pair character, then becomes the $B\,0_u^+$ state discussed here.

D. Comparison of theory and experiment for Au_2

Diatomic gold, particularly in its excited electronic states, provides a severe test for electronic structure theories which claim to be applicable to heavy elements, where relativistic and spin–orbit effects are important (possibly even dominant). To provide a comparison of theory and experiment, Table V lists the experimentally measured and theoretically calculated properties of the ground and excited electronic states of Au_2. The agreement between the measured and predicted electronic state energies is quite good, with the largest error (about 5000 cm^{-1}) occurring in Das and Balasubramanian's calculated energy[25] of the $A\,0_u^+$ state. The bond lengths calculated by these authors are within 0.05 Å of the measured values for all of the electronic states, however, and are somewhat more accurate than the values reported by Ermler *et al.*[24] Perhaps the greatest discrepancies occur for vibrational frequencies. With the exception of the $X\,^1\Sigma_g^+$, $a\,^3\Sigma_u^+$, and $A\,0_u^+$ states the vibrational frequencies reported by Das and Balasubramanian bear little resemblance to those found in the present study. The values calculated for the B and B' states overestimate the experimental results by 19% and 54%, respectively, while the value obtained for the A' state underestimates the experimental value by 24%. Previous work by Ermler *et al.* is no more accurate in this regard, underestimating the frequencies of the B, A, A', and X states by 19%, 15%, 38%, and 14%, respectively. Presumably these errors could be rectified by the use of a more complete basis set or by a more complete treatment of electron correlation. Such a study would be worthwhile, if only to verify that the relativistic effects are being properly treated.

E. Electronic structure of AgAu

The electronic states of AgAu summarized in Table VI are not nearly as well understood as are their Au_2 counterparts. Previous work has been limited to one experimental measurement of the bond strength, giving $D_0^0(AgAu) = 2.06 \pm 0.10$ eV,[7] and some fragmentary references by Ruamps to spectra[5,6] which he has observed. Theoretical investigations provide an estimate of the ionization potential as IP(AgAu) = 8.41 eV,[21] in agreement with our observation of the A–X band system using ArF excimer radiation, which places the ionization potential of AgAu below 9.15 eV.

Equation (4.1) may again be used to predict the separated atom limits to which the A and B states of AgAu dissociate, giving separated atom energies of 9850 and 10 050 cm^{-1} for the A and B states, respectively. From the separated atom limits listed in Table VII for AgAu it is clear that the only possible separated atom asymptote for the A and B

TABLE V. Theory and experiment for Au_2.

State/Parameter	Experiment	Ermler, Lee, and Pitzer[a]	Das and Balasubramanian[b]
$B\,0_u^+$ $T_e(cm^{-1})$	25 685.5[c]	28 630	28 828
$\omega_e(cm^{-1})$	179.85[d]	146	214
$r_e(Å)$	2.5197[c]	2.50	2.549
$B'1_u$ $T_e(cm^{-1})$	24 024.6[e]		26 063
$\omega_e(cm^{-1})$	126.8[e]		195
$r_e(Å)$	2.570[e]		2.536
$A\,0_u^+$ $T_e(cm^{-1})$	19 668.2[f]	21 050	24 605
$\omega_e(cm^{-1})$	142.6[f]	121	145
$r_e(Å)$	2.5669[f]	2.51	2.574
$A'1_u$ $T_e(cm^{-1})$	18 115[e]	21 290	22 055
$\omega_e(cm^{-1})$	223.6[e]	138	170
$r_e(Å)$	···	2.44	2.573
$a\,^3\Sigma_{1u}^+$ $T_e(cm^{-1})$	16 679.8[e]		15 348
$\omega_e(cm^{-1})$	87.8[e]		98
$r_e(Å)$	···		2.776
$X\,^1\Sigma_g^+$ $\omega_e(cm^{-1})$	190.9[d]	165	193
$r_e(Å)$	2.4715[f]	2.37	2.517
$D_e(eV)$	2.29[e,g]	2.27	2.05

[a] Reference 24.
[b] Reference 25.
[c] From Reference 16.
[d] From Reference 6
[e] This work.
[f] From Reference 17.
[g] From Reference 13.

states is the Ag $d^{10}s^1$, $^2S_{1/2}$ + Au d^9s^2, $^2D_{5/2}$ limit at 9161.30 cm^{-1}. Three states which are optically accessible from the ground electronic state arise from this limit. These consist of one $\Omega' = 0^+$ state and two $\Omega' = 1$ states. Our previous observations[1,2] have shown that excited states of the coinage metal dimers with $\Omega' = 1$ tend to have much longer lifetimes than excited states with $\Omega' = 0^+$, which "borrow" oscillator strength from the ion pair state. Based on this observation, it would seem that the A state should be assigned as the $\Omega' = 0^+$ state deriving from the Ag $^2S_{1/2}$ + Au $^2D_{5/2}$ limit, while the B state should be assigned as one of the $\Omega' = 1$ states deriving from this same limit.

Schematic potential energy curves based on the vibrational constants found for the A and B states are given in Fig. 8, along with curves calculated for the Ag^+Au^- and Ag^-Au^+ ion pair states (dashed lines). As in the case of Au_2, the dashed lines are extrapolated from the appropriate separated ion limit using an attractive $-e^2/R$ potential. No corrections for the polarization of one ion by the other, or for Pauli repulsions between closed shells are included. This results in the unphysical behavior that the ion pair curves approach $-\infty$ as $R \to 0$, while the real curves would turn up and become repulsive at some value of R. From the plotted curves it is evident that the Ag^+Au^- ion pair state is expected in the region of the A state. Based on this expectation, we believe that future investigations will reveal that the A state is of 0^+ symmetry, and possesses a sizable electric dipole moment in the sense of Ag^+Au^-. One additional state with $\Omega' = 1$ should be observable in the vicinity of the A and B states, and the analog of the $a\,^3\Sigma_g^+$ state of Au_2 may be observable at frequencies of 15 500–16 000 cm^{-1}. These states have not been located in the present investigation, possibly because the equimolar Cu/Ag/Au alloy is not a good source of AgAu. Since AgAu is more weakly bound than

TABLE VI. Electronic states of $^{107}Ag^{197}Au$.[a]

State	T_0 (cm^{-1})	ω_e (cm^{-1})	$\omega_e x_e$ (cm^{-1})	Lifetime (μs)[b]
B (1?)	24 692.49(116)	92.65(53)	1.06(4)	1.14(5)
A (0^+?)	21 995.97(86)	115.73(18)	0.74(1)	0.040(1)
$X\,^1\Sigma^+$	0.0			···

[a] The vibronic bands listed in Table II were least-squares fitted to the formula $\nu_{v'-0} = T_0 + v'\omega_e' - (v'^2 + v')\omega_e'x_e'$. The resulting values of T_0, ω_e', and $\omega_e'x_e'$ are given here, along with the 1σ error limits (in parentheses) obtained in the fit.
[b] Lifetimes are a weighted average of the values given in Table II.

TABLE VII. Separated atom limits in AgAu.

Separated atom limit				
Silver	Gold	Energy[a] (cm^{-1})	Case (c) states[b]	Case (a) states[b]
$Ag^-, {}^1S_0$	$Au^+, {}^1S_0$	63 908.7	0^+	$^1\Sigma^+$
$Ag^+, {}^1S_0$	$Au^-, {}^1S_0$	42 486.2	0^+	$^1\Sigma^+$
$d^9s^2, {}^2D_{3/2}$	$d^{10}s^1, {}^2S_{1/2}$	34 714.16	$0^+,0^-,1(2),2$	$^1\Sigma^+, {}^3\Sigma^+, {}^1\Pi, {}^3\Pi, {}^1\Delta, {}^3\Delta$
$d^9s^2, {}^2D_{5/2}$	$d^{10}s^1, {}^2S_{1/2}$	30 242.26	$0^+,0^-,1(2),2(2),3$	
$d^9p^1, {}^2P^o_{3/2}$	$d^{10}s^1, {}^2S_{1/2}$	30 472.71	$0^+,0^-,1(2),2$	$^1\Sigma^+, {}^3\Sigma^+, {}^1\Pi, {}^3\Pi$
$d^9p^1, {}^2P^o_{1/2}$	$d^{10}s^1, {}^2S_{1/2}$	29 552.05	$0^+,0^-,1$	
$d^{10}s^1, {}^2S_{1/2}$	$d^9s^2, {}^2D_{3/2}$	21 435.30	$0^+,0^-,1(2),2$	$^1\Sigma^+, {}^3\Sigma^+, {}^1\Pi, {}^3\Pi, {}^1\Delta, {}^3\Delta$
$d^{10}s^1, {}^2S_{1/2}$	$d^9s^2, {}^2D_{5/2}$	9 161.30	$0^+,0^-,1(2),2(2),3$	
$d^{10}s^1, {}^2S_{1/2}$	$d^{10}s^1, {}^2S_{1/2}$	0.00	$0^+,0^-,1$	$^1\Sigma^+, {}^3\Sigma^+$

[a] Atomic energies and ionization potentials taken from Ref. 32; electron affinities taken as EA(Ag) = 10 501.33 cm^{-1} and EA(Au) = 18 620.35 cm^{-1} from Ref. 31.
[b] From Ref. 33.

either CuAu or Au_2, collisions between an AgAu molecule and either a copper or a gold atom can readily lead to displacement reactions of the form

$$AgAu + Cu \rightarrow Ag + AuCu, \tag{4.2}$$

or

$$AgAu + Au \rightarrow Ag + Au_2 \tag{4.3}$$

thereby providing an easy mechanism for destruction of AgAu molecules. A more appropriate alloy source for study of the AgAu molecule would be a silver-rich gold alloy, such as a 2:1 alloy of Ag:Au.

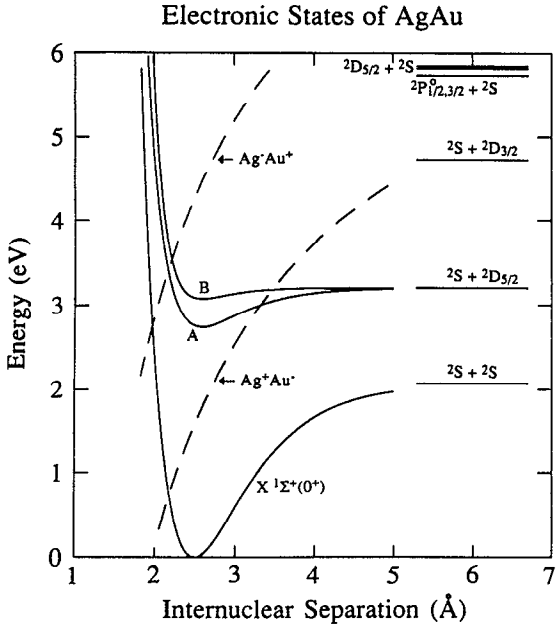

FIG. 8. Qualitative potential energy curves for the experimentally known electronic states of AgAu. Vibrational frequencies and electronic energies are taken from Table VI. Potential curves are plotted as Morse potentials, with anharmonicities adjusted to force dissociation to the appropriate separated atom limits. The ion pair curves for Ag^+Au^- and Ag^-Au^+ are plotted as a dashed lines, without any corrections to account for the polarizability of one ion in the field of the other, or for Pauli repulsion at short distances. Owing to its intensity in absorption and short fluorescence lifetime, the A state is thought to have an electronic symmetry of 0^+, and is believed to correspond to the ion pair state Ag^+Au^-.

V. SUMMARY

The electronic spectra of jet-cooled Au_2 and AgAu have been investigated using the resonant two-photon ionization spectroscopic method, with mass spectrometric detection. Three new band systems of Au_2 have been observed, along with the previously known A–X and B–X systems. The lowest frequency system identified in this work is the $a\,{}^3\Sigma_u^+(1_u) \leftarrow X\,{}^1\Sigma_g^+$ system, which is made observable through spin–orbit contamination of the $a\,{}^3\Sigma_u^+$ state by higher lying $^1\Pi_u$ states. Vibrational levels up to $v' = 33$ have been located, and an extrapolation of these levels gives the bond strength of the $X\,{}^1\Sigma_g^+$ state as $D_0^0(Au_2) = 2.290 \pm 0.008$ eV, in agreement with the results of high temperature Knudsen effusion mass spectrometry. Likewise, the ionization potential of Au_2 has been bracketed as $IP(Au_2) = 9.20 \pm 0.21$ eV, in agreement with the scaled predictions of *ab initio* theory.

The $A'\,1_u$, $A\,0_u^+$, and $B'\,1_u$ states dissociate to the $d^{10}s^1, {}^2S_{1/2} + d^9s^2, {}^2D_{5/2}$ separated atom limit, and are thought to be mostly $^3\Pi_u$ ($\Omega' = 1_u$), $^3\Pi_u$ ($\Omega' = 0_u^+$), and $^1\Pi_u$ in character, respectively. These Π_u states arise from the promotion of a $5d\pi_g$ antibonding electron to the $6s\sigma_u$ antibonding orbital, but are also heavily mixed with other electronic states arising from the same $d^{10}s^1, {}^2S + d^9s^2, {}^2D$ separated atom limit. In addition, the $A\,0_u^+$ state possesses a large oscillator strength in its transitions with the ground $^1\Sigma_g^+$ state, and this is explained as arising primarily from configuration interaction with the $B\,0_u^+$ ion pair state. As in the other coinage metal diatomics, this ion pair state arises from the interaction of a $d^{10}s^0, {}^1S_0$ cation and a $d^{10}s^2, {}^1S_0$ anion, resulting in ion pair states with $\Omega' = 0^+$ (or for homonuclear molecules such as Au_2, $\Omega' = 0_u^+$ and 0_g^+). The transition from the covalent ground state (X) to the ion pair excited state (B) is extremely intense ($f \approx 0.13$), since this is essentially a charge-transfer excitation.

The spectroscopy and electronic structure of the AgAu

molecule has not been investigated as thoroughly as has Au_2, in part because of difficulties in producing the molecule. Nevertheless, two excited electronic states have been located, and assignments of Ω' have been proposed based on the measured decay lifetimes. Both states correlate to the Ag $d^{10}s^1$, $^2S_{1/2}$ + Au d^9s^2, $^2D_{5/2}$ separated atom limit, although the A state is thought to be best described as the Ag^+Au^- ion pair state, based on its short fluorescence lifetime. Future investigations will probably show this state to have a large electric dipole moment, in the sense of Ag^+Au^-.

ACKNOWLEDGMENTS

We thank Professor William H. Breckenridge for the use of the intracavity etalon employed in the high resolution studies, and we thank Jeff Bright for his expert help in preparing the CuAgAu alloy employed in these studies. We also thank Professor Michael Heaven for graciously providing the Franck–Condon routine which allowed the bond length of the B' state of Au_2 to be estimated. We gratefully acknowledge research support from the National Science Foundation under Grant No. CHE-8912673. Acknowledgement is also made to the donors of the Petroleum Research Fund, administered by the American Chemical Society for partial support of this research.

[1] G. A. Bishea, N. Marak, and M. D. Morse, J. Chem. Phys. **95**, 5618 (1991).
[2] G. A. Bishea, J. C. Pinegar, and M. D. Morse, J. Chem. Phys. **95**, 5630 (1991).
[3] M. D. Morse, Chem. Rev. **86**, 1049 (1986).
[4] M. D. Morse, Adv. Metal Semicond. Clusters **1** (in press).
[5] J. Ruamps, Spectrochim. Acta, Suppl. **11**, 329 (1957).
[6] J. Ruamps, Ann. Phys. (Paris) **4**, 1111 (1959).
[7] M. Ackerman, F. E. Stafford, and J. Drowart, J. Chem. Phys. **33**, 1784 (1960).
[8] J. Drowart and R. E. Honig, J. Phys. Chem. **61**, 980 (1957).
[9] J. Drowart and R. E. Honig, J. Chem. Phys. **25**, 581 (1956).
[10] P. Schissel, J. Chem. Phys. **26**, 1276 (1957).
[11] K. Hilpert and K. A. Gingerich, Ber. Bunsenges. Phys. Chem. **84**, 739 (1980).
[12] S. Smoes and J. Drowart, J. Chem. Commun. 534 (1968).
[13] J. Kordis, K. A. Gingerich, and R. J. Seyse, J. Chem. Phys. **61**, 5114 (1974).
[14] J. Ruamps, C. R. Hebd. Seances Acad. Sci. **238**, 1489 (1954).
[15] B. Kleman, S. Lindqvist, and L. E. Selin, Ark. Fys. **8**, 505 (1954).
[16] L. L. Ames and R. F. Barrow, Trans. Faraday Soc. **63**, 39 (1967).
[17] B. Simard and P. A. Hackett, J. Mol. Spectrosc. **142**, 310 (1990).
[18] W. E. Klotzbücher and G. A. Ozin, Inorg. Chem. **19**, 3767 (1980).
[19] R. B. Ross and W. C. Ermler, J. Phys. Chem. **89**, 5202 (1985).
[20] C. W. Bauschlicher, Jr., S. R. Langhoff, and H. Partridge, J. Chem. Phys. **91**, 2412 (1989).
[21] H. Partridge, C. W. Bauschlicher, Jr., and S. R. Langhoff, Chem. Phys. Lett. **175**, 531 (1990).
[22] K. S. Pitzer, Int. J. Quantum Chem. **25**, 131 (1984).
[23] Y. S. Lee, W. C. Ermler, K. S. Pitzer, and A. D. McLean, J. Chem. Phys. **70**, 288 (1979).
[24] W. C. Ermler, Y. S. Lee, and K. S. Pitzer, J. Chem. Phys. **70**, 293 (1979).
[25] K. K. Das and K. Balasubramanian, J. Mol. Spectrosc. **140**, 280 (1990).
[26] S. C. O'Brien, Y. Liu, Q. Zhang, J. R. Heath, F. K. Tittel, R. F. Curl, and R. E. Smalley, J. Chem. Phys. **84**, 4074 (1986).
[27] S. Gerstenkorn and P. Luc, *Atlas du Spectre d'Absorption de la Molecule d'Iode* (CNRS, Paris, 1978); S. Gerstenkorn and P. Luc, Rev. Phys. Appl. **14**, 791 (1979).
[28] K. P. Huber and G. Herzberg, *Molecular Spectra and Molecular Structure IV. Constants of Diatomic Molecules* (Van Nostrand Reinhold, New York, 1979).
[29] P. R. Bevington, *Data Reduction and Error Analysis for the Physical Sciences* (McGraw-Hill, New York, 1969), CURFIT program, pp. 235–45.
[30] G. A. Bishea and M. D. Morse, Chem. Phys. Lett. **171**, 430 (1990).
[31] H. Hotop and W. C. Lineberger, J. Phys. Chem. Ref. Data **14**, 731 (1985).
[32] C. E. Moore, Natl. Bur. Stand. (U.S.) Circ. 467 (US GPO, Washington, D. C., 1949, 1952).
[33] G. Herzberg, *Spectra of Diatomic Molecules* (Van Nostrand Reinhold, New York, 1950), pp. 141–68.